

Control Landscapes for Observable Preparation with Open Quantum Systems

Rebing Wu,^{*} Alexander Pechen,^{*} Herschel Rabitz,^{*} Michael Hsieh,^{*} and Benjamin Tsou^{*}

Abstract

A quantum control landscape is defined as the observable as a function(al) of the system control variables. Such landscapes were introduced to provide a basis to understand the increasing number of successful experiments controlling quantum dynamics phenomena. This paper extends the concept to encompass the broader context of the environment having an influence. For the case that the open system dynamics are fully controllable, it is shown that the control landscape for open systems can be lifted to the analysis of an equivalent auxiliary landscape of a closed composite system that contains the environmental interactions. This inherent connection can be analyzed to provide relevant information about the topology of the original open system landscape. Application to the optimization of an observable expectation value reveals the same landscape simplicity observed in former studies on closed systems. In particular, no false sub-optimal traps exist in the system control landscape when seeking to optimize an observable, even in the presence of complex environments. Moreover, a quantitative study of the control landscape of a system interacting with a thermal environment shows that the enhanced controllability attainable with open dynamics significantly broadens the range of the achievable observable values over the control landscape.

^{*}Department of Chemistry, Princeton University, Princeton, New Jersey 08544, USA

I. INTRODUCTION

Quantum optimal control concepts are being used to address many applications including bond-selective chemical reactions, quantum state engineering, and quantum computation [1, 2, 3, 4, 5, 6]. Toward the natural goal of finding the best attainable outcome, optimal control theory can be applied to redirect the quantum dynamics subject to any practical constraints on the laboratory controls [7]. In the laboratory, optimal control experiments generally have been based on learning algorithms [8] that guide a closed-loop search for an effective control despite the lack of full information about the system’s Hamiltonian, its interaction with the environment and the influence of noise. The growing number of experimental successes [9, 10, 11] collectively show that it is (unexpectedly) easy to find high-quality control results even with severely constrained control fields (i.e., shaped pulses from the same Ti:sapphire laser operating at $\sim 800\text{nm}$ with a bandwidth of $\sim 20\text{nm}$ are used as the driver for most of the experiments).

The quantum control landscape is the expectation value of the physical observable as a functional $J = J[\epsilon]$ of the time dependent control field $\epsilon(\cdot)$. Optimal controls maximize (or minimize, depending on the control goal) the objective functional, i.e., such that $J[\epsilon] = \max_{\epsilon} J[\epsilon]$ (resp., $J[\epsilon] = \min_{\epsilon} J[\epsilon]$). In the laboratory, for controlling a complex system typically detailed knowledge about the dependence of the objective functional on the control is not available, and the practical search for an optimal control solution is performed adaptively via various algorithms (e.g., genetic algorithms, gradient methods). If the objective functional has local traps (local minima or maxima), then their presence can slow down the efficiency of the search or even permanently trap the algorithm in a local maximum (resp., minimum). This circumstance motivates the analysis of the topological properties of quantum control landscapes. In particular, *a priori* information about the absence of local traps for common quantum objective functionals for a wide class of quantum systems would imply that the laboratory searches would not be hindered

and a global optimal solution would be finally reached (assuming that the control field is sufficiently flexible). Moreover, the lack of landscape traps would provide an explanation for the evident relative practical ease of obtaining optimal solutions. Recent studies [12, 13, 14, 15, 16, 17, 18, 19] show that such favorable landscape properties exist for optimizing the expectation value of a system observable for any controllable finite level closed quantum system.

Realistic quantum systems are always exposed to some kind of environment (e.g., chemical reactions in heat baths, or atoms in optical cavities), and their landscape analysis for such systems is important. In most cases, the environmentally induced irreversible quantum dynamics [20, 21] would downgrade the quality of the control outcome, especially when little can be done to tailor the environment. This situation can be serious in many applications, especially quantum information sciences [21]. However, there are indications that it may be possible to fight against or even cooperate with environmentally induced dynamics [22]. Moreover, combining incoherent control by the environment with coherent control by an electromagnetic field offers a general technique for manipulating quantum systems by optimally affecting both the Hamiltonian and dissipative aspects of the dynamics; the latter circumstance corresponds to the environment consisting of incoherent radiation or a gas of electrons, atoms or molecules whose state is suitably optimized [23] (e.g., to allow for the creation of mixed target states). There also have been explicit applications of controlled quantum correlations induced to non-classically manipulate quantum states (e.g., through quantum error correction using redundant qubits [24, 25], atomic control in single-mode optical cavities [26], and real-time feedback control [27, 28]). These scenarios show the prospects of attaining full control of the system evolution by “freezing” or possibly counter-intuitively “reversing” what was thought to be irreversible dynamics [6, 29]. In the laboratory, even if an explicit treatment of the environment is not considered, under optimization of the observable the control will naturally address the environment to maximally draw on its beneficial features or minimize

its deleterious effects to best achieve control of the system.

This perspective forms the background for the present paper aiming to investigate control landscapes of open quantum systems whose dynamics can be effectively manipulated. The landscape analyses will be explored within the framework of the Kraus operator-sum representation of open system dynamics [30], revealing that no local suboptima exist in the control landscape of open systems, although there is an increase of the number of saddle submanifolds from that in the case of analogous closed quantum systems. The open system landscape analysis indicates that the search for optimal controls in the laboratory may not be significantly hindered by the presence of an environment, thereby providing a basis to understand the relative ease of obtaining optimal control of open systems and allowing for the development of more effective searching algorithms.

The paper is organized as follows. Section II summarizes the properties of Kraus maps, while section III presents the concept of landscape lifting and discusses its general aspects. Section IV applies landscape lifting to Kraus maps for manipulation of an observable, thereby revealing a rich structure for the critical submanifolds in the search space and the quantitative influence of the environment on the landscape. Section V summarizes the results.

II. REPRESENTATIONS OF OPEN QUANTUM SYSTEM DYNAMICS

We summarize the Kraus operator-sum formalism of open quantum system dynamics via a simple “system plus environment” model, where the quantum system with Hilbert space dimension N is coupled to an external quantum environment (taken as λ -dimensional), and the composite of the system and the environment obeys the Schrödinger equation,

$$i\hbar \frac{d\rho_{\text{total}}}{dt} = [H_{\text{total}}, \rho_{\text{total}}], \quad (1)$$

where ρ_{total} is the total density matrix. The total Hamiltonian H_{total} includes the internal Hamiltonians of the system and the environment as well as their interaction, all contributing to the total system evolution operator $U_{\text{total}}(t)$ on the total Hilbert space $\mathcal{H} = \mathcal{H}_S \otimes \mathcal{H}_E$, where \mathcal{H}_S and \mathcal{H}_E are the Hilbert spaces of the system and environment, respectively. The composite system is assumed to initially be prepared in a product state $\rho_{\text{total}}(0) = \rho \otimes \varrho$, where ρ and ϱ are the initial states of the system and the environment, respectively. The system dynamics described by $\rho_S(t)$ can be obtained by tracing $\rho_{\text{total}}(t) = U_{\text{total}}(t)\rho_{\text{total}}(0)U_{\text{total}}^\dagger(t)$ over the environment, leading to the Kraus operator-sum representation:

$$\rho_S(t) = \sum_{\alpha, \beta=1}^{\lambda} K_{\alpha\beta}(t) \rho K_{\alpha\beta}^\dagger(t), \quad (2)$$

where $K_{\alpha\beta}(t) = \text{Tr}_E \{U_{\text{total}}(t)(I_N \otimes \varrho^{1/2}|\beta\rangle\langle\alpha|)\}$ is the (α, β) -th $N \times N$ block of the $\lambda N \times \lambda N$ matrix $K = U_{\text{total}}(t)(I_N \otimes \varrho^{1/2})$ under some arbitrary orthonormal basis $\{|\alpha\rangle, |\beta\rangle, \dots\}$ of \mathcal{H}_E . The matrices $\{K_{\alpha\beta}\}$ form the Kraus representation of the dynamical map (2). For compactness, we use K to denote the Kraus representation by the set of Kraus operators $\{K_{\alpha\beta}\}$ associated with the initial environmental state ϱ , which always satisfies the identity

$$K^\dagger K = I_N \otimes \varrho \quad (3)$$

to guarantee that the trace-preservation of the system density matrix [31]. The set of Kraus representations induced by the environment state ϱ is denoted by $\mathbb{K}[\varrho, N]$, which can be taken as the image of the unitary group $\mathcal{U}(\lambda N)$ under the mapping

$$K = \mathcal{F}_\varrho(U) = U(I_N \otimes \varrho^{1/2}), \quad U \in \mathcal{U}(\lambda N). \quad (4)$$

Suppose that the rank of ϱ is μ , then $\mathbb{K}[\varrho, N]$ is homeomorphic to the following homogeneous space of $\mathcal{U}(\lambda N)$

$$\left\{ U \begin{pmatrix} I_{\mu N} & \\ & 0_{(\lambda-\mu)N} \end{pmatrix}, \quad U \in \mathcal{U}(\lambda N) \right\} = \frac{\mathcal{U}(\lambda N)}{\mathcal{U}[(\lambda-\mu)N]}, \quad (5)$$

where each $K \in \mathbb{K}[\varrho, N]$ corresponds to a coset in the unitary group.

The definition (3) of Kraus representation is still ambiguous because the reduction (2) to the system density matrix is dependent on the choice of basis for \mathcal{H}_E . In general, two Kraus operators K and \tilde{K} correspond to the same Kraus map if

$$\sum_{\alpha, \beta} K_{\alpha\beta} \rho K_{\alpha\beta}^\dagger = \sum_{\alpha', \beta'} \tilde{K}_{\alpha'\beta'} \rho \tilde{K}_{\alpha'\beta'}^\dagger, \quad \forall \rho.$$

It is easy to show that the following set of Kraus representations

$$\{\tilde{K} = (I_N \otimes V)K, \quad V \in \mathcal{U}(\lambda)\} \quad (6)$$

are equivalent to K , and they exhaust all equivalent representations when ϱ is a pure state. Here the unitary matrix V represents all possible basis transformations on the environmental subsystem.

Since the sequential order of the Kraus operators in the sum does not affect the operation of Kraus maps on the density matrix, and the effective number of independent Kraus operators is at most N^2 because the Kraus maps are linear in the space of N -dimensional Hermitian operators, any Kraus map can be associated with an N^2 -dimensional “fictitious” environment starting from a pure state. This characterizes the whole set of open system Kraus maps without any explicit environmental details appeared in the formulation. In more general cases, $\mathbb{K}[\varrho, N]$ has to be associated with a specific environment initial state ϱ and the set only involves a proper subset of all possible dynamical maps of the underlying open quantum system.

III. LANDSCAPE LIFTING

The quantum control landscape is defined by a cost functional $J[\varepsilon(t)]$ built on the space of time-dependent control fields that enter into the Hamiltonian H_{total} to manipulate the quantum dynamics. A main objective of the analysis is to determine the topology of the

landscape extremal controls (i.e., critical points of the landscape function) and understand the influence of the topology upon the search for optimal controls.

It can be difficult to carry out a landscape analysis in the space of time-dependent control fields that form a subset of the infinite dimensional space $\mathcal{L}^2(\mathbb{R})$ of Lebesgue integrable functions. However, under some special circumstances with symmetries, the arguments of the functional $J(\cdot)$ may be expressed as a function of a smaller group of variables to define the landscape. For example, consider the state-to-state quantum transition landscape $J[\varepsilon(\cdot)] = |\langle f|U[\varepsilon(\cdot), t_f]|i\rangle|^2$, where $U[\varepsilon(\cdot), t_f]$ is the system propagator at time t_f under control $\varepsilon(\cdot)$ at going from the initial state $|i\rangle$ to the target state $|f\rangle$. The landscape function can be rewritten as $J(U) = |\langle f|U|i\rangle|^2$ over the N^2 -dimensional unitary transformation group manifold $\mathcal{U}(N)$, or more compactly, $J(\psi) = |\langle f|\psi\rangle|^2$ over the unit sphere in the N -dimensional Hilbert space of quantum states $|\psi\rangle$. A general connection between such landscapes is shown by the following theorem:

Theorem 1 *Let $L(x)$ be a landscape defined on some differential manifold \mathcal{X} . If x is a function $x = h(y)$ of y in some other differential manifold \mathcal{Y} with $\dim \mathcal{Y} \geq \dim \mathcal{X}$, and h is locally surjective on a neighborhood of some point $y_0 \in \mathcal{Y}$, i.e., the Jacobian has full rank:*

$$\text{rank } \frac{dh}{dy} \Big|_{y=y_0} = \dim \mathcal{X} \Big|_{x=h(y_0)} \quad (7)$$

in some local coordinate system. Then y_0 is critical for $L \circ h$ in \mathcal{Y} if and only if $x_0 = h(y_0)$ is critical for L in \mathcal{X} , and they have an identical number of positive and negative Hessian eigenvalues at y_0 and x_0 , respectively. Moreover, if the inverse image $h^{-1}(x_0)$ of every critical point x_0 is connected, then the connected components of their critical manifolds are one-to-one between the two landscapes.

Proof: From the chain rule

$$\frac{d(L \circ h)}{dy} = \frac{dL}{dx} \cdot \frac{dh}{dy}, \quad (8)$$

the rank condition (7) guarantees that the gradient of $L \circ h$ vanishes at y_0 if and only if the gradient of L vanishes at x_0 , hence y_0 is critical if and only if x_0 is critical. Moreover, the Hessian quadratic forms at the critical points are related by:

$$\frac{d^2(L \circ h)}{dy^2} = \left(\frac{dh}{dy} \right)^\dagger \cdot \frac{d^2L}{dx^2} \cdot \frac{dh}{dy}.$$

The right hand side is a congruent transformation on the Hessian quadratic form of L at x under the same full-rank condition (7), which preserves the signs of the nonzero Hessian eigenvalues. Provided that the Hessian form is sufficient to determine the types of critical points for both functions, then any maximum (minimum, saddle) point in \mathcal{Y} will be mapped to a maximum (minimum, saddle) point in \mathcal{X} .

Every connected critical manifold of $L \circ h$ in \mathcal{Y} must produce a connected one of L in \mathcal{X} because the mapping $h : \mathcal{X} \rightarrow \mathcal{Y}$ is continuous, so the number of critical components in \mathcal{X} must be no larger than those in \mathcal{Y} . In a general setting, the number of connected components and their simple (multiple) connectedness may not be preserved. Moreover, let y_1 and y_2 belong to two connected critical submanifolds in \mathcal{Y} , respectively, that are mapped into the same point x_0 in a connected critical component in \mathcal{X} . They must lie within the connected component $h^{-1}(x_0)$, which is connected by assumption. Therefore, the two critical submanifolds in \mathcal{Y} can be connected, and hence every connected component in \mathcal{X} must be mapped from a unique connected critical submanifold in \mathcal{Y} , i.e., the connected critical submanifolds in \mathcal{X} and \mathcal{Y} are one-to-one. End of proof.

The rank condition is essential to the viability of lifting the landscape analysis results in a kinematic picture (i.e., on the unitary group irrespective to the system dynamics) to the control landscape on the space of control fields, which has been adopted in prior studies [12, 13, 15]. Here, the full-rank property corresponds to the local controllability along the trajectory driven by some reference control field. If the reference control steers the system propagator to some (kinematic) landscape critical point in $\mathcal{U}(N)$ and local controllability holds, it must also be critical and possess the same optimality status. Such controls are conventionally called regular extremal controls [32]). According to (8),

a rank-deficient landscape lifting can lead to a critical control field as well, which is called a singular extremal control that may have no correspondence to any kinematic critical point in $\mathcal{U}(N)$. So, the critical topology in the space of control fields depends on both regular and singular extremal controls. The optimality of singular extremals can generally be excluded [32, 33], and hence does not affect the search of optimal controls. Therefore, it is sufficient to consider only the normal extremal controls as the inverse image of the kinematic critical points in $\mathcal{U}(N)$ via landscape lifting. This greatly simplifies the landscape analysis by merely working in the kinematic picture.

IV. QUANTUM ENSEMBLE LANDSCAPES OF OBSERVABLE PREPARATION

Theorem 1 provides a useful means to obtain the critical submanifold of an unknown landscape by identifying it with the image of some known landscape via a faithful lifting that satisfies the conditions in Theorem 1. Consider the goal of maximizing the expectation value of the observable θ of an open quantum system with initial state ρ , which can be formulated on the set of Kraus operators:

$$J(K) = \text{Tr} \left(\sum_{\alpha, \beta=1}^{\lambda} K_{\alpha\beta} \rho K_{\alpha\beta}^{\dagger} \theta \right) = \text{Tr} \{ K(\rho \otimes I_{\lambda}) K^{\dagger} (\theta \otimes I_{\lambda}) \}. \quad (9)$$

We can lift this landscape via the mapping (4) to the following landscape over $\mathcal{U}(\lambda N)$:

$$J(U) = \text{Tr} \{ \mathcal{F}_{\varrho}(U) (\rho \otimes I_{\lambda}) \mathcal{F}_{\varrho}^{\dagger}(U) \Theta \} = \text{Tr} (UPU^{\dagger} \Theta), \quad (10)$$

where $P = \rho \otimes \varrho$ and $\Theta = \theta \otimes I_{\lambda}$. Because $\mathbb{K}[\varrho, N]$ is homeomorphic to the homogeneous space of $\mathcal{U}(\lambda N)$ as shown in (5), the properties in the theorem above are naturally guaranteed from the facts that (a) the mapping of a canonical projection is locally surjective [34] and (b) the inverse image of every Kraus operator K is homeomorphic to its coset in $\mathcal{U}(\lambda N)$ and hence is connected. Thus, complete information can be extracted about the

critical landscape topology for open systems from the auxiliary landscape (10), which encompasses the composite “system plus environment” model that targets the maximization of the expectation value of the same system observable (minimization may be treated just as well). We assume that the system is controllable over the set of Kraus maps $\mathbb{K}[\varrho, N]$ generated from an environmental initial state ϱ , while the controllability over $\mathcal{U}(\lambda N)$ is not necessarily as demanding as it might seem in practical physical circumstances since only a portion of the composite system (e.g., just the system and its immediate local environment) is likely required for manipulation. Furthermore, most realistic laboratory control goals will admit as fully acceptable just reaching some reasonable neighborhood of the absolute maximum objective yield.

Note that the controllability criterion does not give any information about the control landscape for open quantum systems, which might be extremely complex in presence of environmental interactions. However, an inherent property revealed about the landscape for open systems can be immediately observed from the above landscape lifting analysis. The open system landscape is always devoid of *false traps* whenever the open system dynamics is fully controllable, because the equivalent landscape for the closed composite quantum system was proven to always possess this basic novelty [16, 19] owing to the linearity and unitarity of quantum system dynamics. This result is of fundamental importance for understanding the evident ease of identifying effective control fields in the presence of uncertainties [8, 9, 10, 11, 12, 15, 18] through the guarantee of not being caught by any false traps using suitable search algorithms in the laboratory with flexible control fields. In addition, the ability to decrease the entropy in the system state shows that open system controlled dynamics can outperform control of the corresponding isolated system without introducing any false traps, as will be seen later.

The details of the landscape topology is affected by the initial environmental state, which can be resolved via the equivalent landscape (10) as well. Other work [19] developed the technique of contingency tables to characterize critical submanifolds. To be specific,

suppose that P has r distinct eigenvalues with degeneracy degrees m_1, \dots, m_r and Θ has s distinct eigenvalues with degeneracy degrees n_1, \dots, n_s . Then every critical submanifold of (10) corresponds to a contingency table shown in Table I.

	n_1	\cdots	n_s
m_1	c_{11}	\cdots	c_{1s}
\vdots	\vdots	\ddots	\vdots
m_r	c_{r1}	\cdots	c_{rs}

Table I: The contingency table of the composite system. The c_{ij} entries satisfy the constraints $\sum_i c_{ij} = m_j$ and $\sum_j c_{ij} = n_i$.

Hence, the determination of critical submanifolds can be reduced to a combinatorial problem of enumerating all possible contingency tables. The dimension and the numbers of positive and negative eigenvalues of the Hessian matrix can also be computed by these contingency tables.

Considering the composite system plus an environment, the marginal conditions can be determined by the degeneracy structures of ρ , ϱ and θ . Suppose that ρ has r distinct non-negative eigenvalues $1 \geq p_1 > \cdots > p_{r-1} > p_r = 0$ with multiplicities d_1, \dots, d_r (d_r can be zero corresponding to no zero eigenvalues in ρ); ϱ has m eigenvalues $1 \geq q_1 > \cdots > q_m = 0$ with multiplicities f_1, \dots, f_m (f_m can be zero corresponding to no zero eigenvalues in ϱ). The distinct eigenvalues of θ are $r_1 > \cdots > r_s$ with multiplicities e_1, \dots, e_s . For simplicity, we assume no accidental degeneracies in $\rho \otimes \varrho$, i.e., $p_i q_j \neq p_k q_\ell$ for arbitrary $1 \leq i \neq k < r$ or $1 \leq j \neq \ell < m$. In this case, the degeneracy structure of the initial state $P = \rho \otimes \varrho$ is

$$D_{11} = d_1 f_1, \cdots, D_{ij} = d_i f_j \cdots, D_{r-1, m-1} = d_{r-1} f_{m-1},$$

corresponding to nonzero eigenvalues $p_i q_j$, where $i = 1, \dots, r$ and $j = 1, \dots, m$, while the zero eigenvalue of P has multiplicity $D_{rm} = d_r \lambda + f_m N - d_r f_m$. The observable $\Theta = \theta \otimes I_\lambda$ possesses the same group of eigenvalues as θ whose degeneracy indices are multiplied by λ , i.e.,

$$E_1 = \lambda e_1, \dots, E_{s-1} = \lambda e_{s-1}, E_s = \lambda e_s.$$

The degeneracy structures define the contingency Table II, where the row and column sums to be satisfied are $(D_{11}, \dots, D_{r-1,m-1}, D_{rm})$ and (E_1, \dots, E_s) .

	E_1	E_2	\dots	E_s
D_{11}	c_{111}	c_{112}	\dots	c_{11s}
\vdots	\vdots	\vdots	\ddots	\vdots
$D_{r-1,m-1}$	$c_{r-1,m-1,1}$	$c_{r-1,m-1,2}$	\dots	$c_{r-1,m-1,s}$
D_{rm}	c_{rm1}	c_{rm2}	\dots	c_{rms}

Table II: The contingency table of the composite system.

A. The Full Control Landscape of Kraus Maps

Consider the control landscape of all possible Kraus maps. As discussed previously, this situation can be equivalently associated with a special N^2 -dimensional environment which is initially in a pure state ϱ that has only one nonzero eigenvalue. The associated contingency Table III shows that P has the same group of eigenvalues as ρ , except for the increase in the number of zero eigenvalues by $N^3 - N$.

	$N^2 e_1 \cdots N^2 e_s$
d_1	$c_{11} \cdots c_{1s}$
\vdots	$\vdots \quad \ddots \quad \vdots$
d_{r-1}	$c_{r-1,1} \cdots c_{r-1,s}$
$d_r + (N^3 - N)$	$c_{r1} \cdots c_{rs}$

Table III: The contingency table for the landscape with pure environmental initial states.

Because of the marginal conditions, the first $r - 1$ rows uniquely determine the contingency table provided that the sum of the first $r - 1$ elements in each column does not exceed the corresponding column sum. This criterion is automatically satisfied in Table III because

$$c_{1j} + \cdots + c_{r-1,j} \leq d_1 + \cdots + d_{r-1} \leq N < N^2 e_j, \quad j = 1, \cdots, s.$$

Thus, the column-sum constraints are actually ineffective, which implies that the number \mathcal{N} of contingency tables depends only on the number of ordered partitions of d_1, \cdots, d_{r-1} , i.e.,

$$\mathcal{N} = \prod_{i=1}^{r-1} \frac{(d_i + s - 1)!}{d_i! (s - 1)!}. \quad (11)$$

The dependence of \mathcal{N} on the degeneracy indices of the nonzero eigenvalues of ρ manifests itself in the contribution of the entropy of the system to the landscape topology. Apparently, the diverse nature of the initial state distributions tends to give rise to more critical submanifolds for large N . The observable θ affects the number of critical submanifolds only by its number of distinct eigenvalues. A physical interpretation of this number is the resolution required to measure the target observable, whose low value facilitates the control and measurement, and hence reduces the complexity of the control landscape despite the environment being present.

Concerning the local topological landscape properties, a prime interest is the number of nonzero eigenvalues at the global optima, which represents the number of effective

search directions close in that neighborhood. The associated contingency Table IV has nonzero entries only in its first column and last row. Applying the formulas developed in [19], we can calculate the number of nonzero Hessian eigenvalues (all negative) as

$$\mathcal{M}_- = 2N^2(N - d_r)(N - e_1).$$

This characteristic is proportional to the number of zero eigenvalues in ρ and the number of eigenvalues smaller than e_1 in the observable θ . Again, the low entropy of ρ helps to reduce the number of search directions towards the global optima, and improves the robustness of this critical manifold. Similarly, the large size e_1 of the eigenspace of the maximal eigenvalue of θ also facilitates the search near the optima.

	N^2e_1	\cdots	N^2e_s
d_1	d_1	\cdots	0
\vdots	\vdots	\ddots	\vdots
d_{r-1}	d_{r-1}	\cdots	0
$d_r + (N^3 - N)$	$N^2e_1 - N + d_r$	\cdots	N^2e_s

Table IV: The contingency table for the global extremum of the open system control landscape.

B. Control Landscapes with a Thermal Environment

This section considers the control landscapes under the common situation that the environment is initially in a thermal equilibrium state

$$\varrho(T) = \frac{\exp(-H_E/kT)}{\text{Tr}[\exp(-H_E/kT)]}, \quad (12)$$

where T is the temperature and k is the Boltzmann constant. For simplicity, we suppose that the environmental Hamiltonian has a non-degenerate spectrum, i.e., $f_1 = \cdots = f_m = 1$. Although under most circumstances the associated Kraus representations do not cover all possible maps, the landscape still exhibits no false traps according to the

analysis. Appendix A estimates the approximate numbers of critical submanifolds under different circumstances. In the limit of zero temperature, the number reaches its maximum value as shown in equation (11), and remains constant when λ is sufficiently large. As the temperature increases, more critical submanifolds grow out from the relatively flat low-temperature landscape. The set of critical submanifolds are identical for all finite temperature values and their number increases exponentially with the size of the environment, while the geometry (e.g., the curvature near the critical submanifolds) varies with the temperature. In the limit of infinite temperature, the landscape critical submanifolds merge into a smaller group whose number increases only polynomially with the size of the environment.

Open system control can also extend the scope of manipulation over the expectation value of the target observable, which is reflected by the dynamical range of the control landscape defined as $\Delta J = J_{\max} - J_{\min}$. For closed systems that evolve from pure states, the attainable landscape values range from the maximal eigenvalue r_1 of the target observable θ to its minimal eigenvalue r_s , i.e., $\Delta J = r_1 - r_s$; the range is usually further restricted in the case of mixed states and in the presence of external disturbances [35]. The dynamical range of open quantum systems may be enhanced through control over the environment and its interactions with the system. Fig.1 examines the dynamical range of a two-level quantum system, where the observable is chosen as the Pauli operator σ_z whose eigenvalues are $r_1 = 1/2$ and $r_2 = -1/2$. The landscape always has the ideal dynamical range $\Delta J_{\max} = 1$ at zero temperature, and shrinks when the temperature increases. Comparing the trends for coupling to different environments, we see that the dynamical range is wider when the open dynamics is fully controllable and when interacting with larger environments. In the limit of infinite temperature, the dynamical range approaches the lower bound for that of the isolated system. In that case the enhanced controllability of the open dynamics benefits the control landscape very little. The distinction between the two groups of curves that differ by the initial system state ρ shows

that lower-entropy helps to extend the dynamical range, i.e., it facilitates higher-quality controls. The degree of attainable control over the environment will be an application specific matter. Importantly, it is reasonable to expect that only the neighboring environment to the system will likely need to be controlled, and this prospect may open up practical conditions for effective use of the environment to aid in the control of system dynamics.

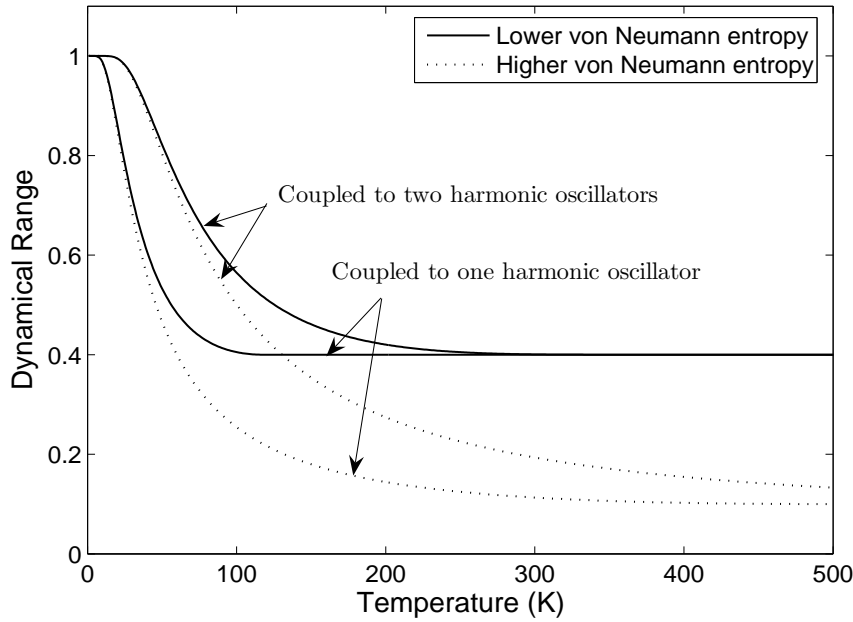


Fig 1: Dynamical range of a two-level system in different thermal environments including one and two harmonic oscillators. The eigenvalues of θ are $r_1 = 1/2$ and $r_2 = -1/2$. The populations of ρ with higher entropy are $p_1 = 0.55$ and $p_2 = 0.45$, while $p_1 = 0.70$ and $p_2 = 0.30$ for ρ with lower entropy.

We illustrate the behavior of the search for optimal dynamical control of the above two-level spin- $\frac{1}{2}$ system interacting with some relatively small environments represented by a spin- $\frac{\lambda-1}{2}$ system (here we choose $\lambda = 6$). The total system Hamiltonian is $H_{\text{total}} =$

$H_0 + \varepsilon(t)\sigma_x \otimes I_\lambda$ with

$$H_0 = \omega_0\sigma_z \otimes I_\lambda + I_2 \otimes \omega_e J_z + \gamma \sum_{\alpha=x,y,z} (\sigma_\alpha \otimes J_\alpha),$$

where the σ 's are the standard Pauli matrices and the spin operators J_x, J_y, J_z form a basis of the $SO(3)$ Lie algebra and possess a λ -dimensional irreducible unitary representation of the $SO(3)$ Lie algebra basis. The environment is initially in a thermal state (12), where $H_e = \omega_e J_z$.

Although the control field only acts directly on the system itself, it can be demonstrated that the rank of the Lie algebra spanned by H_0 and $\sigma_x \otimes I_\lambda$ equals that of the Lie algebra of $\mathcal{U}(2\lambda)$, which implies that the composite system is controllable via the system-environment coupling given a sufficiently large final time [36]. Fig.2 shows the maximization of the cost function (9) using the conjugate gradient algorithm, and the resulting system entropy at each iteration step. As already shown in Fig.1, the dynamical search finds fields that transfer population to the target level beyond the capability of the closed system control landscape at different temperatures. Moreover, the optimal control fields also purify the system as shown in the decrease of the von Neumann entropy in Fig.2. Hence, a clever use of the environment may improve the accessible dynamical range on the system landscape. Fig.3 shows the resulting optimal control field with and without the presence of the environment (i.e., for the case of $T = 300K$). With a relatively small environment, the resonant mode for the state transition arising from the system free Hamiltonian is still dominant in the optimal control field. The entropy in the system state drops slightly more quickly when the temperature of the environment is higher before optimization, i.e., the controlled system becomes cooler when initially bathed in a hotter environment. Although such behavior are physically allowed, the phenomenon is still counter-intuitive. This may be an algorithm and objective-dependent issue with the present goal maximization of the expectation value of θ without any specific consideration of minimizing the system entropy.

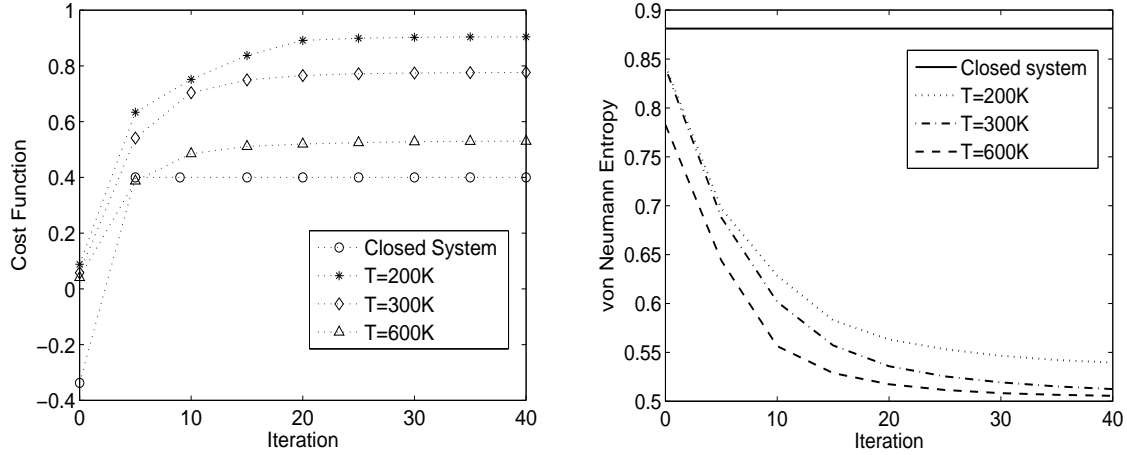


Fig 2: Dynamical search for optimal controls in a two-level open quantum system, where the dimension of the associated environment is $\lambda = 6$. The observable is $\theta = \sigma_z$.

V. CONCLUSION

This work presents an investigation of control landscape topology for open quantum systems. The analysis was performed with the aid of landscape lifting and reveals several inherent properties of the open system control landscapes. The findings here provide a basis to expect that (a) the search for an optimal control in the laboratory may not be significantly hindered by the presence of an environment, (b) no traps exist to limit the control yield, and (c) in favorable cases, the environment can aid the control outcome. These conclusions are consistent with the observed relative ease of attaining control over quantum systems in the laboratory, including those of high complexity in condensed phase environments.

A lack of full controllability may turn some of the saddle critical points for controllable systems into local maxima, and thus generate false traps. Moreover, the influence of singular extremal controls may also be significant when the system is not controllable, because they often appear at the boundary of the reachable set and can become optimal solutions to the control problem. Further studies should take into account such limiting

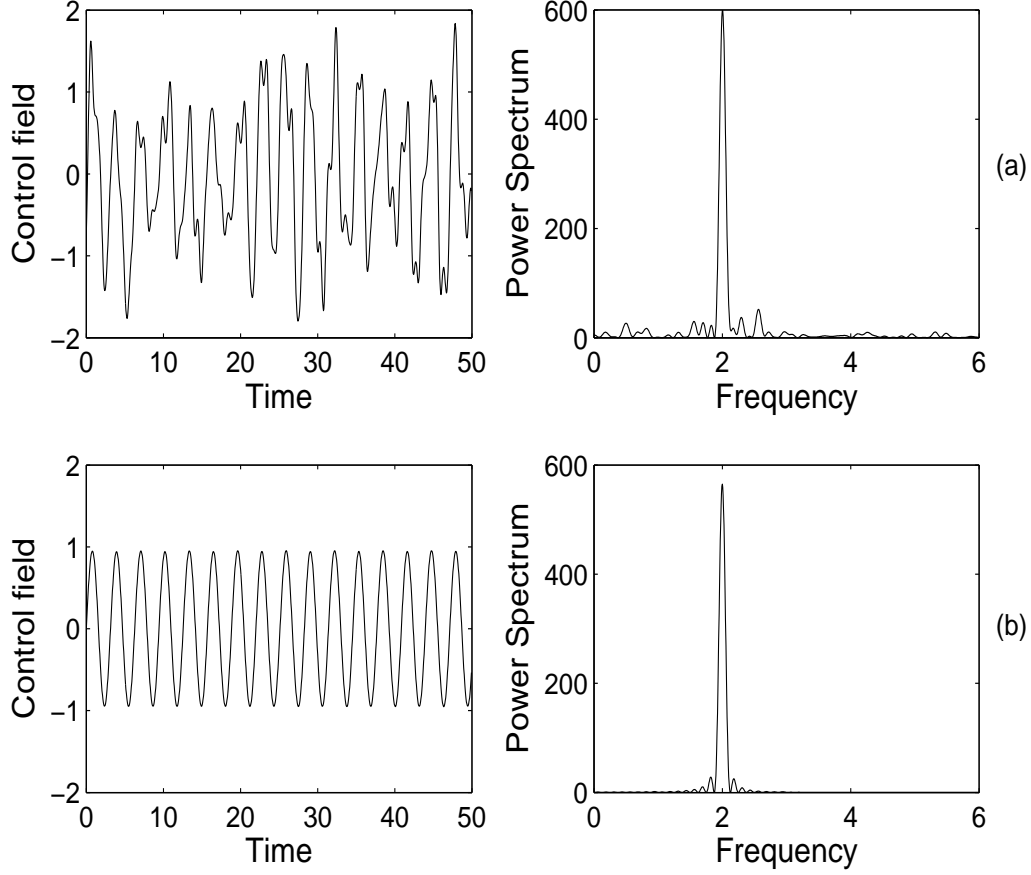


Fig 3: Control fields for open quantum control systems: (a) in presence of the environment initially at temperature $T = 300K$; (b) in absence of the environment.

factors as well as (1) uncontrollable degrees of freedom and (2) the employment of restricted control fields, which might generate apparent false traps in the search for effective controls.

Acknowledgments

The authors acknowledge support from the DOE.

APPENDIX A: ESTIMATION OF THE NUMBER OF CRITICAL SUBMANIFOLDS

An estimate can be given for the number of critical submanifolds, whose precise enumeration is generally NP-hard computable [37, 38]. The following formula matches well to the actual number of critical submanifolds when there are many rows of the contingency table and some of the row sums are large. Suppose that $r \geq s$, i.e., θ has higher degeneracies, then we have the Gaussian formula [39] for the number of critical submanifolds of the isolated system:

$$A_0 \approx \frac{s^{\frac{1}{2}}}{(2\pi\beta)^{\frac{s-1}{2}}} M \exp\left(-\frac{Q}{2\beta}\right), \quad (\text{A1})$$

where

$$Q = \sum_{j=1}^s E_j^2 - \frac{N^2}{s}, \quad M = \prod_{i,j} \frac{(D_{ij} + s - 1)!}{D_{ij}!(s-1)!}, \quad \beta = \sum_{i=1}^r \frac{D_{ij}(D_{ij} + s)}{s(s+1)}.$$

Consider the following circumstances:

(1) For systems with thermal environments at finite nonzero temperature, the marginal sums of the contingency tables are

$$D_{ij} = d_i, \quad E_k = \lambda e_k, \quad i = 1, \dots, r; j = 1, \dots, m; k = 1, \dots, s,$$

from which we obtain the approximate number of critical submanifolds associated with the λ -dimensional thermal environment:

$$A_\lambda \approx \frac{s^{\frac{1}{2}} M_0^\lambda}{(2\pi\lambda\beta)^{\frac{s-1}{2}}} \exp\left(-\frac{\lambda Q}{2\beta}\right), \quad M_0 = \prod_i^{r-1} \frac{(d_i + s - 1)!}{d_i!(s-1)!}. \quad (\text{A2})$$

For large environment dimension λ , the number of landscape saddles increases exponentially with λ .

(2) In the limit of zero temperature, the environmental equilibrium state reduces to a pure state. In this case, the number of critical submanifolds remains constant when λ is sufficiently large, and the precise number is given by the equation (11).

(3) In the limit of infinite temperature, $\varrho_\infty = \lambda^{-1}I_\lambda$ becomes a completely mixed state, which leads to the marginal sums of the contingency tables:

$$D_i = \lambda d_i, \quad E_j = \lambda e_j, \quad i = 1, \dots, r; j = 1, \dots, s.$$

One can show that for large λ ,

$$Q_\lambda = \lambda^2 Q, \quad M_\lambda \approx \prod_{i=1}^r \frac{(\lambda d_i)^{s-1}}{(s-1)!}, \quad \beta_\lambda \approx \lambda^2 \beta,$$

which leads to

$$A_\lambda \approx \left[\frac{s^{\frac{1}{2}} e^{-\frac{Q}{2\beta}}}{(2\pi\beta)^{\frac{s-1}{2}}} \prod_{i=1}^r \frac{d_i^{s-1}}{(s-1)!} \right] \lambda^{(r-1)(s-1)}. \quad (\text{A3})$$

Therefore, the approximate number of critical submanifolds increases polynomially with λ in the limit of infinite temperature.

-
- [1] W. S. Warren, H. Rabitz, and M. Dahleh, *Science* **259**, 1581 (1993).
 - [2] H. Rabitz, R. de Vivie-Riedle, M. Motzkus, and K. Kompa, *Science* **288**, 824 (2000).
 - [3] M. Weitz, *IEEE J. Quantum Elect.* **36**, 1346 (2000).
 - [4] M. Dantus and V. Lozovoy, *Chem. Rev.* **104**, 1813 (2004).
 - [5] V. Bonacic-Koutechy and R. Mitric, *Chem. Rev.* **105**, 11 (2005).
 - [6] L. Viola and S. Lloyd, *Phys. Rev. A* **58**, 2733 (1998).
 - [7] W. Zhu, J. Botina, and H. Rabitz, *The Journal of Chemical Physics* **108**, 1953 (1998).
 - [8] R. Judson and H. Rabitz, *Phys. Rev. Lett.* **68**, 1500 (1992).
 - [9] D. Meshulach and Y. Silberberg, *Nature* **396**, 239 (1998).
 - [10] R. Levis, G. Menkir, and H. Rabitz, *Science* **292**, 709 (2001).
 - [11] T. Bixner, N. Damrauer, G. Krampert, P. Niklaus, and G. Gerber, *J. Modern Optics* **50**, 539 (2003).
 - [12] H. Rabitz, M. Hsieh, and C. Rosenthal, *Science* **303**, 1998 (2004).
 - [13] H. Rabitz, T. Ho, M. Hsieh, R. Kosut, and M. Demiralp, *Phys. Rev. A* **74**, 12721 (2006).
 - [14] H. Rabitz, M. Hsieh, and C. Rosenthal, *J. Chem. Phys.* **124**, 204107 (2006).
 - [15] T.-S. Ho and H. Rabitz, *J. Photochemistry Photobiology A* **180**, 226 (2006).
 - [16] M. Hsieh, R. Wu, and H. Rabitz, to be submitted (2007).
 - [17] A. Rothman, T.-S. Ho, and H. Rabitz, *Phys. Rev. A* **72**, 23416 (2005).
 - [18] H. Rabitz, M. Hsieh, and C. Rosenthal, *Phys. Rev. A* **72**, 52337 (2005).
 - [19] R. Wu, M. Hsieh, and H. Rabitz, submitted to *J. Phys. A* (2007).
 - [20] R. Alicki, in *Irreversible Quantum Dynamics* (Springer-Verlag, Trieste, Italy, 2003), pp. 121–39.
 - [21] M. Nielsen and I. Chuang, *Quantum computation and quantum information* (Cambridge University Press, Cambridge, 2000).

- [22] F. Shuang, M. Dykman, and H. Rabitz, J. Chem. Phys. **121**, 9270 (2004).
- [23] A. Pechen and H. Rabitz, Phys. Rev. A **73**, 062102 (2006).
- [24] C. Bennett, Int. J. Theor. Phys. **42**, 153 (2003).
- [25] D. Cory, M. Price, W. Maas, E. Knill, R. Laflamme, W. Zurek, T. Havel, and S. Somaroo, Phys. Rev. Lett. **81**, 2152 (1998).
- [26] T. Wellens and A. Buchleitner, in *Dynamics of dissipation*, edited by P. Garbazezski and R. Olkiewicz (Springer-Verlag, 2002), pp. 351–376.
- [27] J. Geremia, J. Stockton, and H. Mabuchi, Science **304**, 270 (2004).
- [28] R. van Handel, J. Stockton, and H. Mabuchi, IEEE Trans. Automat. Contr. **50**, 768 (2005).
- [29] R. Brockett, C. Rangan, and A. Bloch, in *Proceedings of the 42th IEEE Conference on Decision and Control* (Hawaii, U.S.A., 2003), pp. 428–433.
- [30] A. Pechen, D. Prokhorenko, R. Wu, and H. Rabitz, to be submitted (2007).
- [31] K. Kraus, Annals of Physics **64**, 311 (1971).
- [32] B. Bonnard and M. Chyba, *Singular trajectories and their role in control theory* (Springer-Verlag, Berlin, 2003).
- [33] R. Wu and H. Rabitz, in preparation (2007).
- [34] S. Helgason, *Differential geometry, Lie groups, and symmetric spaces* (American Mathematical Society, Providence, 2001).
- [35] M. Girardeau, Physical Review A **58**, 2684 (1998).
- [36] V. Ramakrishna, M. V. Salapaka, M. Dahleh, H. Rabitz, and A. Pierce, Phys. Rev. A **51**, 960 (1995).
- [37] E. Bender, Discrete Math. **10**, 217 (1974).
- [38] M. H. Boon and T. H. Seligman, J. Math. Phys. **14**, 1224 (1973).
- [39] M. Gail and N. Mantel, J. Amer. Statist. Assoc. **72**, 859 (1977).